Commun Nonlinear Sci Numer Simulat 19 (2014) 83–91

Contents lists available at SciVerse ScienceDirect

Commun Nonlinear Sci Numer Simulat

journal homepage: www.elsevier.com/locate/cnsns

Multi-scale entropy analysis of vertical wind variation series in atmospheric boundary-layer

Zuntao Fu *, Qinglei Li, Naiming Yuan, Zhenhua Yao

Dept. of Atmospheric and Oceanic Sciences, Laboratory for Climate and Ocean-Atmosphere Studies, School of Physics, Peking University, Beijing 100871, China

ARTICLE INFO

Article history:
Received 27 October 2011
Received in revised form 17 May 2013
Accepted 19 June 2013
Available online 3 July 2013

Keywords:
STI
MSE
Non-stationary
Eddy organization

ABSTRACT

Turbulent vertical wind variation records in atmospheric boundary-layer have been analyzed in this study. By means of space time-index (STI for short) method, vertical wind variation records can be classified as stationary and non-stationary. And then among these vertical wind velocity records, ten most stationary and ten most non-stationary records are chosen as two contrast groups for further analysis. Multi-scale entropy (MSE for short) analysis has been applied to quantify the increments of these two groups of wind-velocity records with different time lags. And marked differences are detected between non-stationary and stationary series, the entropy for the increments of stationary vertical wind records is larger than that of non-stationary ones when the time lags are smaller. So over certain range with small values of scale factor, the MSE can be taken as an indicator to quantify the different levels of eddy organization between the stationary turbulent vertical wind records and those non-stationary ones.

1. Introduction

The atmospheric boundary layer is inherently non-stationary, turbulence time series collected in the atmospheric surface layer over land may often be non-stationary. It has been found that a stationarity test shows that about 40% of the turbulent heat fluxes at Summit, Greenland are classified as non-stationary. Three main factors are explored to account for the large fraction of non-stationary runs: (1) intermittency of turbulence in stable conditions, (2) changes in net all-wave radiation in response to cloud forcing, and (3) diurnal trends in stability [12].

The related concepts of stationarity and the existence and values of integral time scales are central to the ability of analyzing micrometeorological data within the framework of Monin–Obukhov similarity theory and other classical analysis. However, issues related to non-stationarity are not well understood and have only recently received more attention (e.g. Gluhovsky and Agee [15]; Dias et al. [13]; Mahrt [24,25]). We know little about how to handle or even to judge non-stationarity that we cannot make progress in determining its consequences without a better way to characterize it.

Usually, the non-stationarity is closely linked to the coexistence of eddies of various scales, especially the coherent structures, in the turbulent flow. In studies of atmospheric turbulence, coherent structures are used to denote the distinct large-scale fluctuation patterns regularly observed in a given turbulent flow [31]. In the Ref. [1], the authors found that the preferred regime produces both first-order and second-order non-stationarity, which manifests a change in the series mean and in the variance for a segment of time series, is for the mean to increase while the variance simultaneously decreases. Such behavior is taken as evidence of coherent structures, often seen as ramps [2]. The ramp patterns in scalar traces such as temperature and vapor have been reported both in the unstably stratified surface layer and in the stably stratified

* Corresponding author. Tel.: +86 010 62767184; fax: +86 010 62751094.
E-mail address: fuzt@pku.edu.cn (Z. Fu).

1007-5704/$ - see front matter © 2013 Elsevier B.V. All rights reserved.
http://dx.doi.org/10.1016/j.cnsns.2013.06.026

surface layer, observations reveal the distinctive features of ramp structure in the turbulence records and surrounding the ramp are the regions of relatively quiescent fluctuations. Therefore, the issue of non-stationarity is also closely related to studies describing the occurrences of intermittent turbulence [14,24], where intermittency is characterized by brief episodes of turbulence with intervening periods of relatively weak or small fluctuations of motion. In order to explain the turbulence intermittency, the synchro-cascade pattern theory [34] proposed that eddies of various sizes coexist and interweave with each other in each step of the cascade in the space occupied by the fluid, and their nonlinear interaction with each other strengthens or weakens their amplitudes. Thereby the interaction between eddies of various sizes causes strong fluctuations in amplitude with different scales, and then forms intermittency in the fluid turbulence. So the degree of organization of complex eddy motions of various scales is really crucial to the non-stationarity of fluid turbulence.

In this paper, we will seek to quantify the different degrees of organization of complex eddy motions using nonlinear dynamics method to contrast the non-stationarity effect in the vertical wind velocity (w) time series collected in the atmospheric surface layer (ASL). The wind in the atmospheric boundary layer is known to be distinctively turbulent and non-stationary. As a consequence the wind velocity varies rather randomly on many different time scales. In order to capture their multi-scale features, we will adopt the multi-scale entropy to quantify the differences resulted from the different degrees of organization of complex eddy motions, i.e. the non-stationarity effect.

The rest of the paper is organized as follows. In Section 2, we will make a short introduction of the analysis methods and the data sets we used. Results for relationship between Shannon entropy distribution and increments of different scales for stationary and non-stationary turbulent vertical wind-velocity series are provided in Section 3. In Section 4, we make some discussion and the conclusions are summarized.

2. Data and methodology

2.1. Data

In this paper, atmospheric boundary-layer turbulence records collected during the experiment in Huaihe River Basin (HUBEX) between June 5 and June 22 in 1998 are used in the analysis. Huaihe River basin is situated between Yangtz River and Yellow River with a total area of 270,000 km^2. It represents the typical climate condition in the East Asia monsoon region, and effects of human activity are relatively slight. The observation site was in the yard of the Shouxian Meteorological Observatory in Anhui province, People's Republic of China and is located on the western edge of a large rice field. The yard was about 200 m long in the north–south direction. The measurement height was set as 4 m above ground, a three-dimensional sonic anemometer (SAT- 211/3 K, sample rate 20 Hz, sound path 0.15 m) was used to measure wind velocity components and temperature, and each hour sampling will be taken as one record (detailed information can be found in the references [9,10]). And this data set has been applied to analyze the characteristics of turbulence in the atmospheric boundary-layer, and nonlinear features have been derived [9,10,20,28]. Typical parts of records can be found in the Fig. 1, where stationary and non-stationary, original or normalized (subtracting mean value and divided by standard deviation) records show the different features, especially there are dominant larger scale structures in the non-stationary record, see Fig. 1(b).

2.2. Identify the non-stationarity in turbulence series and space time index (STI) method

First of all, we need the stationary and non-stationary records to contrast the effect of non-stationarity on the features of turbulence series. However, the meteorological community has no consensus definition of what non-stationarity is and thus no consensus method for how to identify it [1]. Many methodologies have been applied to test the records' stationarity, such as the Run Test (RUT) and the Reverse Arrangement Test (RAT), whose details can be found in Bendat and Piersol [4, pp. 94–99]. Both tests are nonparametric and able to detect trends, but less so to detect non-stationary behavior of the kind, for example, of a sine fluctuation [15]. The RAT, a more powerful test for detecting trends than RUT according to Bendat and Piersol, its test rationale is the same as for the RUT, but they often disagree in detecting non-stationarity [13]. An examination of the accuracy of the RUT, RAT and modified RAT for assessing stationarity of signals finds that both the stationary and non-stationary signals were tested for stationarity using the RUT, RAT and modified RAT, and each of the three stationarity tests demonstrated at least one form of inaccuracy in examining the stationarity of the test signals. These findings may reflect the fact that these tests were designed to determine whether or not a signal is random, and to identify drift or the presence of a trend (s) in data, rather than examine signal stationarity exclusively. Thus, RUT, RAT and modified RAT may not be appropriate for assessing stationarity considered signals [3]. So in this paper, we will use space time-index (STI) method to identify whether a record is stationary or non-stationary, since it has been shown that STI method can determine a record whether stationary or not accurately [19]. STI was first proposed by Yu et al. in 1998 [32]. In 1999, this method was modified in Ref. [33]. In this study, we choose the modified STI as our detection methods to classify the records of turbulent vertical wind velocity in the atmospheric boundary-layer. Here we will make a brief introduction of this method. Suppose we have an observed time series of length N, with equidistant time interval. First of all, normalize the data into a range (0,1) to generate a new series $F:\{s_i|i=1,2,\ldots,N\}$. Then, the series is divided into two segments A and B with the same length, $A:\{s_i|i=1,2,\ldots,N/2\}$ and $B:\{s_i|i=N/2+1,N/2+2,\ldots,N\}$. Secondly, embed F,A and B into an m-dimensional phase space using delay coordinates with a delay time η, and create state vectors F^m,A^m and B^m.

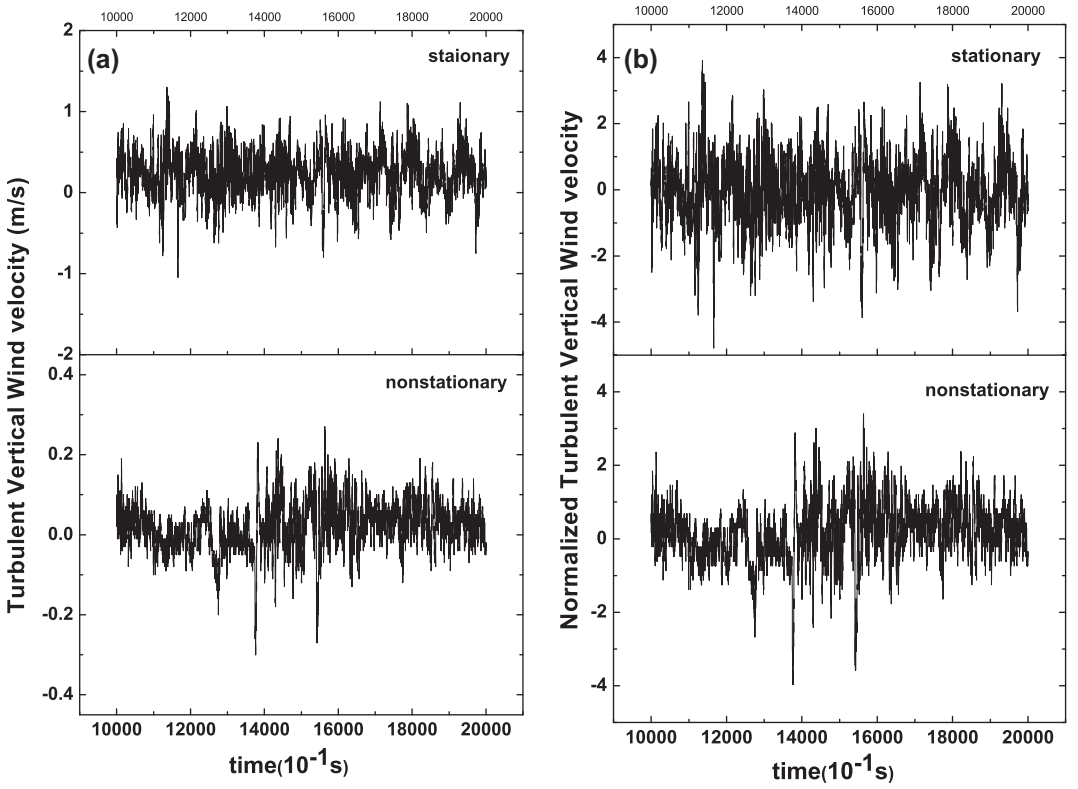

Fig. 1. Parts of stationary (up) and non-stationary (bottom) wind series, (a) is for original series and (b) is for normalized series.

$$A^m : \{x_i = [s_i, s_{i+\eta}, \ldots, s_{i+(m-1)\eta}]^T | i = 1, 2, \ldots, N_A\}$$
$$B^m : \{y_i = [s_{i+N/2}, s_{i+N/2+\eta}, \ldots, s_{i+N/2+(m-1)\eta}]^T | i = 1, 2, \ldots, N_B\}$$
$$F^m : \{z_i = [s_i, s_{i+\eta}, \ldots, s_{i+(m-1)\eta}]^T | i = 1, 2, \ldots, N_F\}$$

where η is delay time, the superscript T denotes transpose of a vector and $N_A = N_B = N/2 - (m-1)\eta, N_F = N - (m-1)\eta$. Thirdly, define the time-index D between two points x_i and x_j $(i \neq j)$ as

$$D = T(x_j) - T(x_i) = j - i, \quad \text{if } j > i$$

$$D = N - T(x_i) + T(x_j) = N - j + i, \quad \text{if } j < i$$

where $T(x_i) = i$ stands for the time location i of the point x_i along the trajectory. For a reference point x_i in set F^m, we can find all its near neighbors within a given space distance $\varepsilon, \|x_j - x_i\| < \varepsilon$. Calculate all time indices between x_i and x_j, accumulate the population $N_s(D)$ for each time-index $D, N_s(D) \to N_s(D) + 1$, and repeat the procedure for all reference points x_i, then we can get the auto-time index populations $N^{FF}(D)$. Similarly, we can get the other two auto-time index populations $N^{AA}(D), N^{BB}(D)$ and two cross-time index populations $N^{AB}(D), N^{BA}(D)$. At last, bin the five populations into $K+1$ intervals between the minimum and maximum time-index, and create normalized distribution functions, $\rho^{FF}(\zeta)$, $\rho^{AA}(\zeta), \rho^{BB}(\zeta), \rho^{AB}(\zeta)$ and $\rho^{BA}(\zeta)$, respectively.

$$\rho(\zeta) = \frac{N(\zeta)}{N_t}, \tag{1}$$

where $\zeta \in (0, K)$ is the normalized time-index, $N_t = \sum_D N_s(D)$. The time series is considered to be stationary if and only if $\rho^i(\zeta) = \rho^{ii}(\zeta)$ (the superscripts i and ii represent any two of the five distribution functions) and all distribution functions $\rho(\zeta)$ are constant, independent of ζ. Otherwise, the time series is considered to be non-stationary. The typical results can be found in the Fig. 2(a), where all distribution functions $\rho(\zeta)$ are constant, independent of ζ for stationary records; whereas all distribution functions $\rho(\zeta)$ for non-stationary record are not constant, see Fig. 2(b). Generally, we use χ^2 test to examine these two conditions. For more details, please refer to Refs. [32,33].

Based the above results, from all observational records, we can select 20 records by the STI method, ten of them are the most non-stationary and the other ten are the most stationary. Some statistics, such as dates and times of measured records; mean values of the vertical velocity $\overline{u}$; the variance of w, σ_w^2; the mean temperature $\overline{T}$ and other variables were calculated and listed in the Table 1. These variables include the friction velocity u_*,

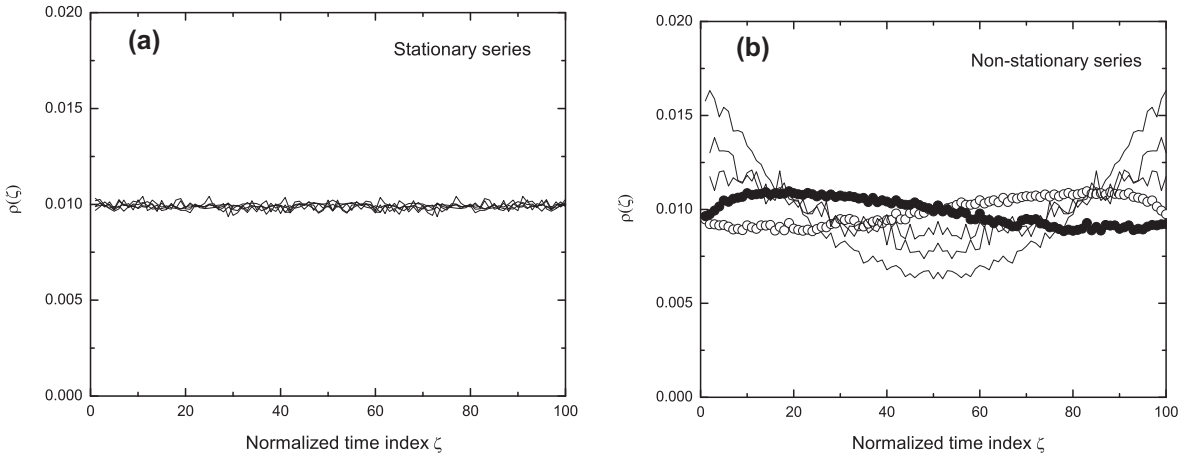

Fig. 2. Distributions of the normalized distribution functions $\rho^{FF}(\zeta), \rho^{AA}(\zeta), \rho^{BB}(\zeta)$, $\rho^{AB}(\zeta)$ and $\rho^{BA}(\zeta)$ of proxy time series, (a) is the results of stationary series generated by Henon map; (b) is the results of non-stationary series generated by Baker's map.

Table 1
Values and mean values of measured variables for the selected 20 samples.

Date and time	STI	z_m/L	$\overline{u}(ms^{-1})$	$u_*(ms^{-1})$	$\sigma_w^2(m^2s^{-2})$	$H(Wm^{-2})$	$\overline{T}(^\circ C)$
06-11 02:00	ST	1.39	1.33	0.05	0.01	−4.35	23.65
06-11 05:00	ST	0.13	2.50	0.18	0.07	−18.03	23.68
06-11 06:00	ST	0.04	3.09	0.18	0.10	−5.79	23.88
06-11 20:00	ST	0.18	2.06	0.13	0.04	−9.85	28.92
06-11 07:00	ST	−0.04	3.19	0.22	0.10	12.05	24.23
06-11 11:00	ST	−0.44	3.89	0.25	0.16	163.19	27.74
06-11 13:00	ST	−2.07	8.29	0.15	0.19	193.21	29.87
06-11 17:00	ST	−0.04	6.75	0.23	0.09	12.85	30.85
06-12 11:00	ST	−0.21	2.33	0.16	0.07	22.02	26.24
06-12 17:00	ST	−0.02	−1.52	0.35	0.36	25.30	24.65
06-09 23:00	NON	2.50	0.48	0.02	0.002	−0.62	23.83
06-10 04:00	NON	3.44	0.17	0.02	0.002	−0.51	22.68
06-15 01:00	NON	0.16	1.24	0.10	0.02	−4.07	24.52
06-15 20:00	NON	14.79	−0.05	0.01	0.004	−0.36	30.18
06-17 23:00	NON	0.30	0.93	0.08	0.016	−4.01	27.88
06-10 22:00	NON	2.94	0.69	0.03	0.003	−1.81	24.87
06-13 17:00	NON	2.37	−0.33	0.01	0.001	-0.15	22.49
06-10 07:00	NON	−1.89	0.40	0.03	0.005	1.62	23.21
06-14 02:00	NON	−3.52	0.26	0.01	0.001	0.01	21.78
06-14 16:00	NON	−0.48	2.66	0.17	0.09	58.46	28.66

$$u_* = \left[\overline{u'w'}^2 + \overline{v'w'}^2\right]^{1/4}; \tag{2}$$

the Obukhov length

$$L = -\frac{u_*^3\overline{T}}{\kappa g\overline{wT'}} \tag{3}$$

and the sensible heat flux,

$$H = \varrho c_\varrho \overline{wT'}, \tag{4}$$

where $\overline{x}$ and $x\prime$ symbolize the time averaging and deviation from the mean of a measured variable x, u and v are the longitudinal and transversal wind velocity, respectively, T is atmospheric temperature, $\kappa(=0.4)$ is the von Karman constant, g is the acceleration due to gravity, ϱ is the density of air, and c_ϱ is the specific heat capacity of air. Atmospheric stability is denoted by $\xi = z/L$, and usually $-0.02 < \xi < 0.02$ means neutral stratification, $-0.02 \geqslant \xi$ unstable stratification and $\xi \geqslant 0.02$ stable stratification.

The two kinds of records can be classified as two groups, stationary (STI labels as ST in Table 1) and non-stationary (STI labels NON in Table 1). Before using these two kinds of records to further analyze the different behaviors between non-stationary and stationary vertical wind velocity in atmospheric boundary-layer, we first make power spectrum analysis

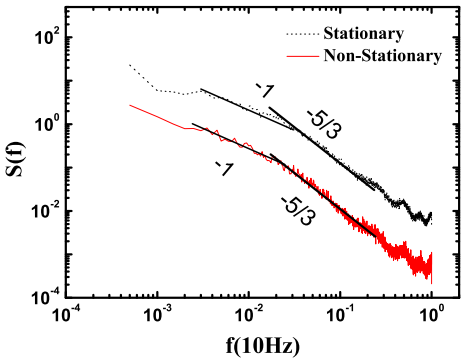

Fig. 3. Power spectrum analysis of the stationary and non-stationary wind velocity series (vertical shift has been taken for clarity). The solid black straight lines represent the behavior over certain ranges, the numbers denotes the slope of the solid lines.

on them by Fast Fourier Transform (FFT) method. The results are shown in Fig. 3. Just as the usual horizontal scaling analysis on the wind velocity in the boundary layer, there are two dominant scaling ranges in the power spectrum of vertical velocity series, both stationary and non-stationary. Over the higher frequency range, the slope of the power spectrum is close to the classical Kolmogorov scaling exponent $-\frac{5}{3}$, this has been reported in the earlier literature [17,27]. Over lower frequency range, the slope of the power spectrum is close to scaling exponent -1, which has also been found in the wall-bounded turbulence studies [17]. Although coherent structures or large-scale motions interacting with inertial size eddies weakens universal signature of f^{-1} scaling behavior over lower frequency range, we can not find the quantitative difference from power spectrum of vertical velocity series between stationary and non-stationary series. Another feature in the power spectrum analysis of vertical wind velocity series is that the Bolgiano-Obukhov scaling behavior with exponent $-\frac{11}{5}$ [6], which has been found both in the vertical scaling studies [18,22] and thermal convection turbulence [5,26], is not found over a dominant range.

2.3. Quantifying the effect of the non-stationarity and multi-scale entropy (MSE) analysis

Nonlinear time series analysis has been used by Wesson et al. [29] to quantify the organization of atmospheric turbulent eddy motion, one of nonlinear dynamics methods sensitive to distinct measures of organization of a given time series is Shannon or information entropy [30], which is defined as

$$I_s = -\sum_i p_i \log p_i \tag{5}$$

$p_i (i = 1, 2, \ldots M)$ is a discrete probability distribution. For further calculations, we will use the normalized Shannon entropy, $S_N = I_s / \ln(M)$ where M is bin number. S_N is guaranteed to be between 0 and 1, and this normalization ensures that entropy differences attributed to different sampling lengths and duration are minimized [29]. Using this definition of the Shannon entropy provides a technique that gives information about the order or disorder of the flow. For example, when flow is dominated by organized structures with a certain scale and then most of the energy of the spectrum resides at a peaked, small wave-number band. This will produce a very small Shannon entropy value. If the organization of the flow decreases, the energy shifts to smaller scales and the shape of the spectrum becomes less peaked and more flattened. In this case, the complexity of the flow increases and the Shannon entropy, correspondingly, becomes larger. The largest possible value of the Shannon entropy is obtained when the signal becomes characterized by a flat, white noise spectrum. Wesson's study concluded that the more intense the organization of the flow, the lower the value of the Shannon entropy. Eddies in the atmospheric turbulent motion are usually multi-scaled, so only Shannon entropy calculated from the original record can't fully quantify the multi-scale features. Here in this study, we will consider the velocity increment with different time lags used in structure function analysis to quantify the attributes from multi-scale eddies. The velocity increment reads

$$\delta v_i^\tau = v(i + \tau) - v(i), \tag{6}$$

where τ is the time lag. Next, we calculate the normalized Shannon entropy for each normalized velocity increment with different time lags, and call it multi-scale entropy (MSE). In this study, we apply this method to quantify different properties between stationary and non-stationary turbulent vertical wind velocity records.

3. Results and analysis of turbulent vertical wind velocity

3.1. Non-stationary characteristics

First of all, we can see the obvious difference between the stationary and non-stationary turbulent vertical wind velocity records from the observational series directly, see Fig. 4, where both the original records and their increment records with

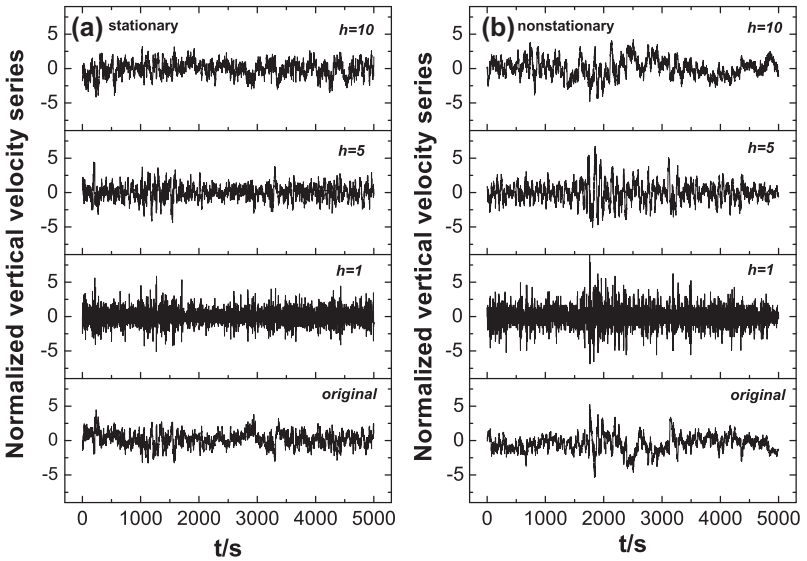

Fig. 4. Typical normalized original wind series and its increment series with different scale factors ($h = 1, h = 5$ and $h = 10$), (a) is for stationary series and (b) is for non-stationary series.

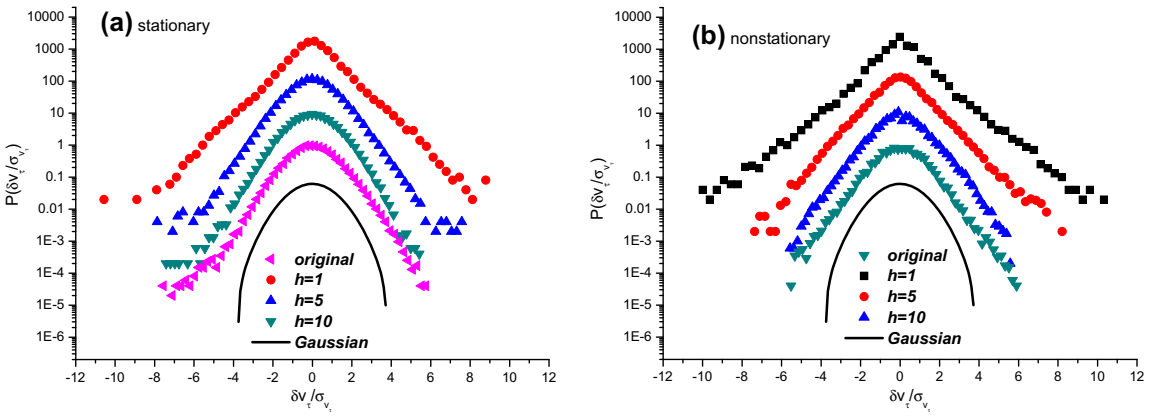

Fig. 5. PDF for the original wind series and its increment series with different scale factors ($h = 1, h = 5$ and $h = 10$), (a) is for stationary series and (b) is for non-stationary series.

different scale factors, where scale factor h defined as $\tau = 2^h$, $h = 0, 1, 2, \ldots, 10$, have been presented. For the original records, compared to stationary wind velocity variations, there are more dominant large scale structures in the non-stationary ones. These kinds of large scale eddies can also be found in their increment records with large or small scale factors, for example, when $h = 1$ or $h = 5$, there are more clusterings of larger amplitude events in the non-stationary increment variations than stationary ones. When the scale factor arrive at $h = 10$, the dominant large scale structures recover in the non-stationary increment variations. All these results indicate that there are different levels of organizations of eddy motion between stationary and non-stationary vertical wind variations.

In fact, this kind of difference between stationary and non-stationary vertical wind variations can also be found in their probability distributions, see Fig. 5. It is obvious that the probability distribution function (PDF) for wind velocity variations and their increment fluctuations is marked different between stationary and non-stationary records. The PDFs of stationary wind variations and their increment fluctuations with larger scale factors, such as $h = 10$, are close to Gaussian distributions, which are those found in the homogeneous, isotropic and stationary turbulent laboratory flows. For the non-stationary wind velocity increment fluctuations, however, PDFs differ from above PDFs. With the scale factors decrease, PDFs of increments are characterized by marked fat tails [11,16,21] and/or a peak around the mean value. They are much more intermittent and do not approach a Gaussian distribution even for very large scales. Large increment values in the tails directly correspond to

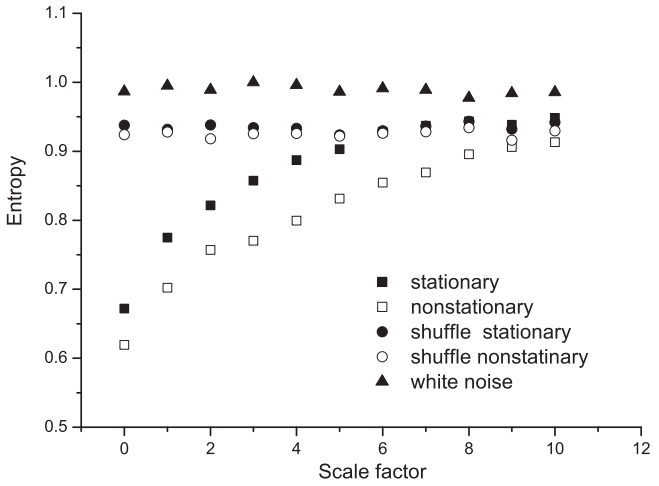

Fig. 6. Relationship between Shannon entropy and scale factor h. The hollow box and the solid box correspond to the results of non-stationary and stationary series, respectively. The hollow circle and the solid circle represent the results of the non-stationary and stationary series after shuffling procedure, respectively. The solid triangle represents the results of white noise.

an increased probability to observe large and very large events. These marked difference has been found by Boettcher's group [7,8] and they thought that these marked intermittency of probability density functions of velocity increments can be understood as a superposition of different subsets of isotropic turbulence caused by non-stationarity of atmospheric winds [7].

3.2. Multi-scale entropy analysis

Next, we will quantify the differences between stationary and non-stationary velocity increments by the MSE. The above differences between stationary and non-stationary velocity increments from the observational records and PDFs are more descriptive or qualitative, in order to deeply understand their differences, we need the quantitative results. The Shannon entropy can quantify these differences, and it has been applied by Wesson [29] to quantify key attributes about the degree of organization of complex eddy motion in the atmospheric surface layer (ASL) and the canopy sublayer (CSL). They found that the vertical velocity in the CSL is more organized than in the ASL, which indicates that the organized eddies must be originating from a flow instability whose signature remains persistent, such as a mixing layer in the CSL. Their findings are interesting, however, there are still more problems unsolved, such as mixing layers are known to have a long memory in the sense that the instability mode remains the energetic mode as more eddy sizes are produced and dissipated. How these eddies of different sizes interact each other? And what is difference from that the mode of instability originating from interactions between the surface and the fluid is rapidly distorted by an entire population of new eddies? Especially the interactions between eddies of different scales from different mechanisms should be quantified. We will address this issue by using MSE, since it can be used to quantify the interactions between eddies of different scales.

The MSE is applied to the two contrast groups of selected stationary and non-stationary vertical wind velocity records and the results are shown in the Fig. 6. First of all, we can see that on the same scale factor, the normalized Shannon entropies of stationary wind increments are all larger than that of non-stationary ones, this indicates that the eddies are more organized in the non-stationary than in the stationary conditions. Secondly, with the scale decreasing, the normalized Shannon entropies are all dropping quickly for both stationary and non-stationary wind increments. This is corresponding to the considerably deviation from the Gaussian distribution on the small scales found on the Fig.5. Also this low normalized Shannon entropies can be caused by long-term memory in the original records, the stronger persistent correlation and the lower values of the normalized Shannon entropies [35]. Thirdly, the scale on which instability mode remains the energetic mode in the stationary winds are much smaller than in the non-stationary flows. The normalized Shannon entropy for stationary winds will reach its saturation level on the much smaller scale, such as $h = 6$, but for non-stationary winds, the normalized Shannon entropy still doesn't arrive at its saturation level even when $h = 10$.

These larger scale structures and persistent correlations will be lost when the whole original records are randomly shuffled [23], where this transformation preserves the amplitude distribution of the original records, but eliminates any autocorrelation (equivalently, changes the power spectrum to a white noise spectrum). The corresponding normalized Shannon entropies for both stationary and non-stationary wind increments are nearly the same on each scale and reach their saturation level, see Fig. 6. At the same time, we can see that the saturated normalized Shannon entropies are a bit smaller than those of white noise process (equal to 1) on each scale. This is caused by the slight deviation from the Gaussian white noise process for the atmospheric turbulent wind variations, especially for the large fluctuations on small scales.

4. Conclusion and discussion

The wind in the atmospheric boundary layer is known to be distinctively turbulent and non-stationary. As a consequence, the wind velocity varies rather randomly on many different time scales. One of the most striking features is the PDFs of the observed atmospheric increment show robust (stretched) exponential tails that decay faster than a power-law and slower than a Gaussian distribution [7,8,11,16,21]. Nevertheless, for most technical and meteorological problems fluctuations as well as fluctuation differences are assumed to obey Gaussian statistics, and this will cause confusion on understanding the atmospheric turbulence. In this paper we focus on the scale dependent statistics of atmospheric wind increments and contrast the features between stationary and non-stationary wind increments. First of all, based on the dynamical detection method, STI, we selected 10 extreme stationary and 10 extreme non-stationary records to construct two contrast samples. From them, we can found the descriptive difference between two groups directly from the observational records, and there are more large scale structures and large fluctuations on the small scales in the non-stationary wind variations. This will lead to a transition from Gaussian distributions to intermittent (heavy-tailed) ones as scale decreases. At the same time, we may think the non-stationary wind variations are resulted from the organization level of eddy with different scales. And we use MSE to learn the links between these eddy structures and quantitatively measure the organization level of eddies with different scales for the stationary and non-stationary wind variations. It is found that the eddies are also more organized in the non-stationary wind variations. It is worth mentioning that the normalized Shannon entropy values of original series are similar between stationary and non-stationary winds. But the MSE difference is significant between the velocity increment variations, over certain ranges with small values of scale factor. Different coherent structures with different scales and their interactions result in these differences, since there are different coherent structures with different scales in the stationary turbulent vertical wind velocity records from those non-stationary ones.

The cause leading to the different normalized Shannon entropy values of the vertical velocity increment variations between stationary and non-stationary winds is complicated, and it may not stem from a sole mechanism. From the Table 1, it can found that there are 3 from 10 samples are under stable stratification, 4 from 10 samples are under near-neutral stratification and 3 from 10 samples are under unstable stratification for stationary case but there 3 from 10 samples are under unstable stratification and 7 from 10 samples are under stable stratification for the non-stationary case. This may indicate that the stratification is not the only major factor determining the value of the normalized Shannon entropy as suggested in Ref. [29], there are still other factors which can contribute to the measured records' non-stationarity, such as changes in radiation [12], gravity waves [25] and so on.

Acknowledgement

Many thanks are due to supports from National Natural Science Foundation of China (No. 40975027). The valuable comments and suggestions from the anonymous reviewers are appreciated and helpful in further improving the manuscript.

References

[1] Andreas EL, Geiger CA, Trevino G, Claffey KJ. Identifying nonstationarity in turbulence series. Boundary Layer Meteorol 2008;127:27.
[2] Antonia RA, Chambears AJ. Note on the temperature ramp structure in the marine surface layer. Boundary Layer Meteorol 1978;15:347.
[3] Beck TW, Housh TJ, Weir JP, et al. An examination of the runs test, reverse arrangements test, and modified reverse arrangements test for assessing surface EMG signal stationarity. J Neurosci Methods 2006;156:242.
[4] Bendat JS, Piersol AG. Random data: analysis and measurement procedures. 2nd ed. New York: John Wiley & Sons; 1986.
[5] Boffetta G, De Lillo F, Mazzino A, Mussacchio S. Bolgiano scale in confined Rayleigh–Taylor turbulence. J Fluid Mech 2012;690:426.
[6] Bolgiano R. Turbulent spectra in a stably stratified atmosphere. J Geophys Res 1959;64:2226.
[7] Bottcher F, Barth St, Peinke J. Small and large scale fluctuations in atmospheric wind speeds. Stoch Environ Res Risk Assess 2007;21:299.
[8] Bottcher F, Benner CH, Waldl HP, Peinke J. On the statistics of wind gusts. Boundary Layer Meteorol 2003;108:163.
[9] Chen HY, Chen JY, Hu F, Zeng QC. The coherent structure of water vapour transfer in the unstable atmospheric surface layer. Boundary Layer Meteorol 2004;111:543.
[10] Chen J, Hu F. Coherent structures detected in atmospheric boundary-layer turbulence using wavelet transforms at Huaihe river basin, China. Boundary Layer Meteorol 2003;107:429.
[11] Cheng XL, Zeng QC, Hu F. Characteristics of gusty wind disturbances and turbulent fluctuations in windy atmospheric boundary layer behind cold fronts. J Geophys Res 2011;116:D06101.
[12] Cullen NJ, Steffen K, Blanken PD. Nonstationarity of turbulent heat fluxes at Summit, Greenland. Boundary Layer Meteorol 2007;122:439.
[13] Dias NL, Chamecki M, Kan A, Okawa CMP. A study of spectra, structure and correlation functions and their implications for the stationarity of surface-layer turbulence. Boundary Layer Meteorol 2004;110:165.
[14] Doran JC. Characteristics of intermittent turbulent temperature fluxes in stable conditions. Boundary Layer Meteorol 2004;112:241.
[15] Gluhovsky A, Agee E. A definitive approach to turbulence statistical studies in planetary boundary layers. J Atmos Sci 1994;51:1682.
[16] Guo H, Chen JJ, Qu QL, Liu PQ. Generation of spatial atmospheric turbulence field in aircraft motion simulation based on refined similarity hypothesis. Sci China 2011;54:244.
[17] Katul GG, Porporato A, Nikora V. Existence of k_{-1} power-law scaling in the equilibrium regions of wall-bounded turbulence explained by Heisenberg's eddy viscosity. Phys Rev E 2012;86:066311.
[18] Lazarev A, Schertzer D, Lovejoy S, Chihirinskaya Y. unified multifractal atmospheric dynamics tested in the tropics part II, vertical scaling and generalized scale invariance. Nonlinear Processes Geophys 1994;1:115.
[19] Li QL, Ma N, Fu ZT. Comparative analysis of detection methods of non-stationarity in time series. Acta Sci Nat Univ Pekin 2013;49:252.
[20] Li X, Hu F, Liu G. Characteristics of chaotic attractors in atmospheric boundary-layer turbulence. Boundary Layer Meteorol 2001;99:335.
[21] Liu L, Hu F, Cheng XL, Song LL. Probability density functions of velocity increments in the atmospheric boundary layer. Boundary Layer Meteorol 2010;134:243.
[22] Lovejoy S, Tuck AF, Hovder SJ, Schertzer D. Is isotropic turbulence relevant in the atmosphere. Geophys Res Lett 2007;34:L15802.

[23] Lucio JH, Valdes R, Rodriguez LR. Improvements to surrogate data methods for nonstationary time series. Phys Rev E 2012;85:056202.
[24] Mahrt L. Intermittency of atmospheric turbulence. J Atmos Sci 1989;46:79.
[25] Mahrt L. Stratified atmospheric boundary layers. Boundary Layer Meteorol 1999;90:375.
[26] Shangand XD, Xia KQ. Scaling of the velocity power spectra in turbulent thermal convection. Phys Rev E 2001;64:065301.
[27] Szilagyi J, Katul GG, et al. The local effect of intermittency on the inertial subrange energy spectrum of the atmospheric surface layer. Boundary Layer Meteorol 1996;79:35.
[28] Wang JY, Fu ZT, Zhang L, Liu SD. Information entropy analysis on turbulent temperature series in the atmospheric boundary-layer. Plateau Meteorol 2005;24:38.
[29] Wesson KH, Katul GG, Siqueira M. Quantifying organization of atmospheric turbulent eddy motion using nonlinear time series analysis. Boundary Layer Meteorol 2003;106:507.
[30] Wijesekera HW, Dillion TM. Shannon entropy as an indicator of age turbulent overturns in the oceanic thermocline. J Geophys Res 1997;102:3279.
[31] Wilczak JM. Large-scale eddies in the unstably stratified atmospheric boundary surface layer. Part I velcoity and temperature structure. J Atmos Sci 1984;41:3537.
[32] Yu D, Lu W, Harrison RG. Space time-index plots for probing dynamical nonstationarity. Phys Lett A 1998;250:323.
[33] Yu D, Lu W, Harrison RG. Detecting dynamical nonstationarity in time series data. Chaos 1999;9:865.
[34] Zhao SN. A new turbulence energy cascade pattern and its scaling law. Europhys Lett 2005;69:81.
[35] Zunino L, Soriano MC, Rosso OA. Distinguishing chaotic and stochastic dynamics from time series by using a multiscale symbolic approach. Phys Rev E 2012;86:046210.